Missouri University of Science and Technology
Scholars' Mine

Symposia on Turbulence in Liquids | Chemical and Biochemical Engineering

01 Jan 1973

Statistical Analysis of Instantaneous Velocities in Turbulent Flow of Dilute Viscoelastic Solutions

A. L. Rollin

F. A. Seyer

Follow this and additional works at: https://scholarsmine.mst.edu/sotil

 Part of the Chemical Engineering Commons

Recommended Citation

Rollin, A. L. and Seyer, F. A., "Statistical Analysis of Instantaneous Velocities in Turbulent Flow of Dilute Viscoelastic Solutions" (1973). *Symposia on Turbulence in Liquids*. 102.
https://scholarsmine.mst.edu/sotil/102

This Article - Conference proceedings is brought to you for free and open access by Scholars' Mine. It has been accepted for inclusion in Symposia on Turbulence in Liquids by an authorized administrator of Scholars' Mine. This work is protected by U. S. Copyright Law. Unauthorized use including reproduction for redistribution requires the permission of the copyright holder. For more information, please contact scholarsmine@mst.edu.

STATISTICAL ANALYSIS OF INSTANTANEOUS VELOCITIES IN TURBULENT FLOW OF DILUTE VISCOELASTIC SOLUTIONS

A. L. Rollin, Ecole Polytechnique de Montreal
2500 Avenue Marie-Guyard, Montreal 250, Quebec, Canada
F. A. Seyer, Department of Chemical Engineering, University of Alberta,
Edmundton,Alberta, Canada

ABSTRACT

An experimental study, based on streak photograph determination of instantaneous velocities, was directed at determining the structure of turbulence within the boundary layer and core regions of circular pipes. The measurements lend support to the ejection phenomenon as the mechanism controlling drag reduction.

A correlation factor, defined as the ratio of the observed number of positive instantaneous radial velocities, to the observed number of negative instantaneous radial velocities, suggests acceleration in the radial direction as the elements of fluid move through the sublayer. The correlation factor also provides information about the thickening of the boundary layer for drag reducers relative to the Newtonian case.

Radial turbulent intensity data for 0.01% aqueous solutions of Separan AP-30 were found to be markedly lower, at all radial positions, than the intensities for Newtonian fluids. The lowering of the radial intensities being ordered according to the amount of drag reduction.

INTRODUCTION

Since Prandtl developed the Boundary Layer Hypothesis in 1904 many studies of properties of Newtonian turbulence (10,12,5,15,26,7,9,23) have indicated that the character of the flow in the wall region was responsible for most of the creation and dissipation of the turbulent energy.

It is only recently that a detailed physical picture of the mechanism has been obtained and presented by Bakewell and Lumley (1), Kline, et al. (14), Corino and Brodkey (2) and Nychas (19). Bakewell and Lumley indicated that the dominant large scale structure of the flow in the boundary layer consists of randomly distributed, counter-rotating, longitudinal pairs of eddies elongated in the flow direction. The structure of these eddies was inferred from space-time correlation functions of the fluctuating velocities. The picture of streamlines of these eddies resulted in pushing of low momentum boundary layer fluid toward the core region, resulting in a renewal of fluid by flow in the circumferential direction.

Qualitatively similar patterns of flow in the wall region were visualized by Kline et al. using a dye injection technique, and more detail was obtained from tracer photograph techniques by Corino and Brodkey and Nychas. Ejections of fluid, originating from a low velocity region adjacent to the viscous sublayer, were responsible for extracting energy from "lumps" of fluid originating in the main flow and converting it into turbulent energy. They observed that these ejections were of large scale and moved through the boundary layer until broken down by mixing with the main flow.

The mechanism of turbulence, then, is apparently that the turbulent shear stress is generated by the radial transport of low momentum fluid by the eddies or "bursts". The magnitude of the stress is determined by the rate of radial fluid transport as well as its axial momentum. The rate of the radial transported fluid in turn, depends on the frequency

of occurrence of the eddies as well as their size. Thus, visual studies of turbulence near the wall provide a starting point for interpreting turbulence measurements in drag reduction systems.

Various mechanisms have been suggested in order to explain drag reduction for flow of viscoelastic fluids in pipes (20,26). Generally, it is agreed that the elasticity of the fluid is responsible for drag reduction. Furthermore, the Wells and Spangler (30) technique of injection of polymer in the boundary layer showed that drag reduction is controlled by the flow in the wall region. It is believed that the fluid elasticity directly affects the turbulence near the wall.

It is difficult to predict what the effect of viscoelasticity is on the wall eddy structure. For example, the eddies may be increased in size which would result in a thickening of the boundary layer. Alternatively a reduction of their frequency, would have a similar result. These points of view have resulted in dimensionless groups (4,28) which are basically the same as obtained for the stretching arguments (16,11), but which do not show conclusively what changes in the structure have occurred.

PROBABLE MECHANISM

The recent physical interpretation of turbulence, presented by Corino and Brodkey, based on the observation of a "bursting phenomenon" in the wall region, can serve as a basis to analyze the data of this work. Figure 1 shows schematically a portion of fluid originating in the main flow and entering at a small angle into the boundary layer. It has an axial velocity component corresponding to, or greater than, the average velocity of its origin. A second lump of fluid located in the boundary layer and possessing a lower velocity (lower than the incoming lump velocity) is then accelerated by the intrusion of the first lump, and momentum is transferred until one or more ejections occur. Because ejections are assumed to originate in a region of low momentum situated approximately at a Y^+ of 10 in a Newtonian fluid, the axial velocity components of the ejections are expected to be smaller than those of the incoming lumps. Corino and Brodkey observed that the ejected fluid, although accelerated in the axial direction, never reached the axial velocity of the main flow adjacent to the boundary.

Denoting u_{x1} and u_{r1} as the velocity components of the portion of fluid entering the boundary layer and u_{x2} and u_{r2} for the ejection velocity components, one should expect to find

$$\bar{u}_{x1}(r) > \bar{u}_{x2}(r), \qquad (1)$$

where $$\bar{u}_x(r) = \frac{1}{n}\sum_{i=1}^{n}(u_x(r))_i$$

is the time-average velocity at a fixed radial position if sufficient readings are taken (of instantaneous velocities) at random times.

Each positive (directed toward the wall) radial velocity is associated with a u_{x1} while a negative radial velocity is associated with u_{x2}. The velocity measurements can then be ordered according to whether the instantaneous radial velocity is positive or negative. According to the bursting model, instantaneous negative radial velocities should be larger in magnitude than the positive components. Thus to obtain a zero time-averaged radial velocity (the sum of all observed components) the positive components must be observed more often than the larger negative components.

Defining $$R_o = n^+/n^-, \qquad (2)$$

where n^+ is the observed number of u_{r1}
n^- is the observed number of u_{r2},

then R_o is expected to be greater than unity in the boundary layer and approximately equal to unity in the core region. Also, if the ejection velocity is dependent on radial position, as Corino and Brodkey observed, then an acceleration of the fluid to a radial position where it is broken up by the main flow, implies the presence of a peak in the plot of R_o versus dimensionless radial position. This peak should occur in the vicinity of the edge of the boundary layer.

In summary, an analysis of the axial and radial components of the instantaneous velocities at a radial position in the boundary layer should provide information about the mechanism of ejection.

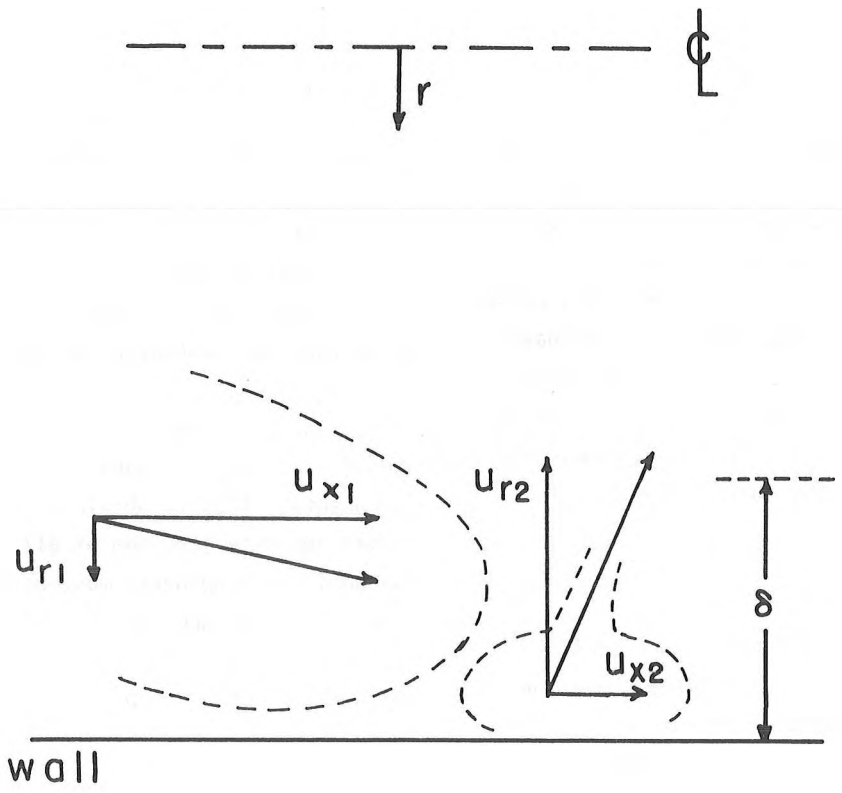

Figure 1. Illustration of Bursting Process

For drag reducers the available data, although doubtful quantitatively, show that the turbulence is similar to Newtonian fluid turbulence. The drag reduction, therefore, is probably a result of modifications to the ejection process. For example, if the boundary layer is thickened appreciably, then the peak in R_o ought to appear at greater values of Y^+ than in the Newtonian case.

Earlier studies (5,27) suggest the increased resistance to stretching of viscoelastic fluids causes the radial fluctuations to decrease. Although one of these studies (27) treated the ideal case of steady stretching, the same conclusion follows from a consideration of the transient motion. Referring to Figure 1 it is seen that an increase of resistance to sudden deformations would: a) decrease u_{r2} at a given point, b) not affect appreciably u_{r1} and u_{x1}, because the direction of these larger lumps of fluid is nearly parallel to the flow direction (negligible stretching in the axial direction), c) implies a lower radial variance from a combination of a) and b) (u_{r1} not affected and u_{r2} decreased). One cannot predict the change in u_{x2} but if a decrease results, as might be expected if the sublayer thickens appreciably, then a higher axial intensity would result.

Similarly the data of Donohue, et al. (6), Meek and Baer (16) and Fortuna and Hanratty (9), show the frequency of ejection occurrence decreases in polymer solutions. This would also decrease the radial intensity of turbulence. Unfortunately, the data obtained in the present work are not extensive enough to distinguish directly whether a change in frequency is effective in altering the intensity or whether it is due to marked reductions in the magnitude of the fluctuations themselves.

EXPERIMENTAL

Instantaneous velocities were obtained by photographing small air bubbles (approximately 0.002 in. diam.) in 1-in. and 2.75-in. tubes for water and 0.01% by weight of aqueous solutions of Separan AP-30. The apparatus used was an improved version of that used in a similar study (28) and allowed measurements to be made significantly closer to the wall and also to obtain significantly larger statistical samples of the fluctuating velocities (23).

Test Sections and Optical Assembly

The two test sections consisted of 30ft of 1-in. ID precision bore pyrex tube and 36.1 ft. of 2.75-in. ID Plexiglas pipe. Fluid from a 300 gal. stainless steel tank was supplied to the test sections with a 2L10H Moyno pump and metered with a 2-in. Foxboro magnetic flow meter. Entry lengths of 187 L/D and 114 L/D were provided for the small and large tubes, respectively. Pressure drop measurements over successive sections of pipe which were obtained with ordinary manometers, indicated the flow was well developed at the position where velocities were measured.

The optical assembly employed a 300 Watt high pressure Xenon arc lamp as a light source. The light source was interrupted with a slotted timing wheel which provided streaks of known duration of about 1/2400 sec. This speed was sufficiently high to ensure that all components of the fluctuating velocities were sampled (23). The view section of the 1-in. tube consisted of a Plexiglas box surrounding the pipe and filled with a mineral oil in order to match refractive indices.

For the Plexiglas pipe, the square view section approximately 12-in. long, was machined from a solid piece of Plexiglas and mounted between two sections of pipe. After the view section had been connected, the upstream joint between the two sections was polished smooth to remove any discontinuity that would disturb the flow. Streak photographs were obtained on 35 mm Tri-X film using various lenses as determined by the test section and/or portion of the tube cross-section under consideration. The magnification on the film was approximately 2X and 8X for the core and wall regions, respectively. The film negatives were subsequently back-projected on a glass screen to an overall magnification of from 40X to 160X. Streak lengths in the axial direction at known radial positions were then measured using a X-Y facility which automatically converted the information and provided a punched card (digitizer). Overall magnification of the system in the axial direction was defined by photographs of a precision steel rule projected onto the

screen. Radial magnifications which include any effects owing to optical distortion, were determined in a similar fashion by photographing the tip of a fine needle that could be positioned relative to the wall with a precision micrometer.

For each of the runs in Table I, a series of approximately 300 photographs was obtained with a high magnification lens combination to define the flow in the wall region. The field of view extended from the wall to radial positions somewhat in excess of $y^+ = 30$. Calibration photographs in the radial direction and axial direction were then obtained. The lenses were changed to a lower (2X) magnification such that the field of view extended to the centerline, and another series of approximately 200 photographs defining the flow in the core region, was obtained. The calibration procedure was repeated for the low magnification system. Each photograph contained several streaks at random radial positions. Streaks crossing preselected radial positions were then measured as described in the following section. This procedure resulted in roughly 30 to 40 observations for each radial position in the wall region and roughly 50 to 100 observations for positions outside the wall region. A more complete description of the experimental apparatus can be found elsewhere (23).

Analysis of Streak Photographs

All photographs were analyzed using the digitizer. Figure 2 shows schematically a projected photograph containing a single streak. The large arrows represent the interrupted streak and its direction for a period corresponding to the time taken by three spokes of the timing wheel to cut the light. The lines parallel and perpendicular to the wall represent the axial and radial components of the velocity for one time period of the streak.

In order to determine the streak length in the axial and radial directions for a known period, readings of four coordinates relative to the fixed frame of the digitizer were needed. Points 1 and 2 represent the beginning and end of a streak-spoke, respectively, and points 3 and 4 locate the line determining the pipe wall and consequently the axial and radial directions of the pipe. With these readings and the appropriate calibrations, the resolution of a streak into a radial and an axial component follows directly.

The dashed lines represent the band defining a radial position where the streaks were classified as acceptable. The true radial position for each acceptable streak was taken to be the location of the center of the band. In the core region, where the velocity and intensity gradients are small, the width of the band is of little consequence. However, this is not true near the wall. For the average velocity near the wall, since the profile is essentially linear over the width of the band, the average is not changed. However, the calculated intensity will be slightly higher than the actual intensity as discussed below.

Generally, if two or more correlated streak patterns were observed in the band on the same photograph, only one reading of the velocity was taken. This was done to eliminate the bias of too many readings of the same instantaneous velocity.

Knowing the time scale and length scale for each streak-spoke, the axial and radial instantaneous velocities could be found:

$$u_x(r) = \Delta x / T \tag{3}$$

$$u_r(r) = \Delta r / T$$

The mean velocities could then be calculated, at a radial position

$$\langle \bar{u}_x \rangle = \frac{1}{n} \sum_{1}^{n} (u_x)_i \tag{4}$$

$$\langle \bar{u}_r \rangle = \frac{1}{n} \sum_{1}^{n} (u_r)_i ,$$

and the Root-Mean-Square values calculated from

$$S_x = \sqrt{\frac{\sum_{1}^{n} (\bar{u}_x - u_x)_i^2}{n - 1}} \tag{5}$$

$$S_r = \sqrt{\frac{\sum_{1}^{n} (\bar{u}_r - u_r)_i^2}{n - 1}}$$

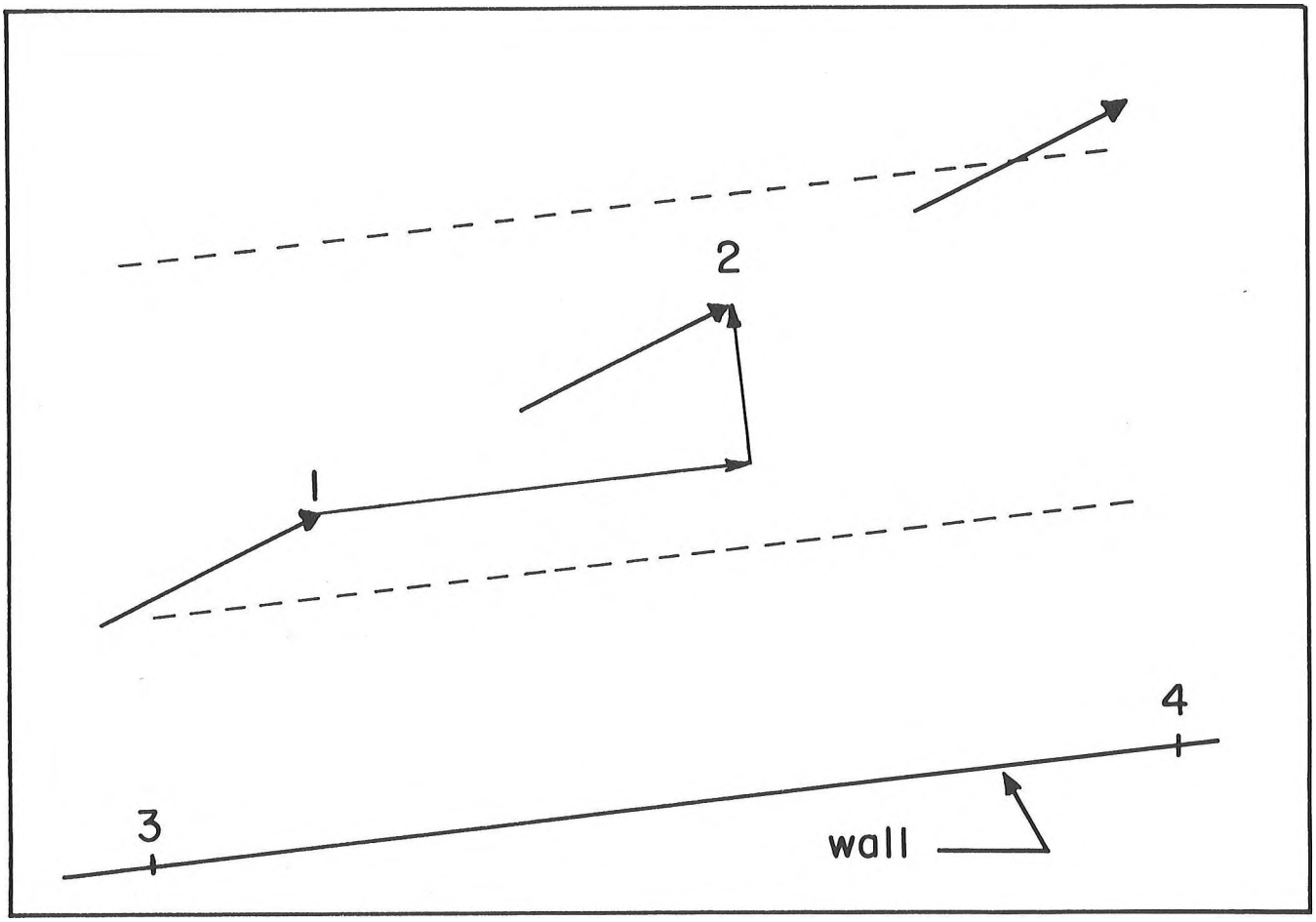

Figure 2. Interpretation of Streak Photograph

Error Analysis

As discussed by Seyer (27), the influence of the air bubbles on the intensity measurements will be negligible if their size is smaller than the scale of the energy containing eddies (approximately 0.006 in.). In this work the average bubble diameter was 0.002 in. and no influence is expected.

The fact that velocities were taken over a band of position rather than a single radial position causes the calculated intensities to be too high. This occurs because the mean velocity gradient causes the observed velocities (streak length) at the bottom of the band (nearest to wall) to be, on the average, slightly smaller than the observed velocities near the top. Thus there is a fluctuation in velocity owing to variations in the radial position of the streaks. The magnitude of the error depends on the velocity gradient as well as the width of the band.

A conservative estimate of the error in the calculated intensity can be obtained by assuming the streaks are located either at the center or top or bottom of the band. In fact there will be a distribution of positions which peaks at the center of the band. In the following sketch the positions $y + \Delta y$ and $y - \Delta y$ represent the limits of the band for a radial position y. Acceptable streaks were:

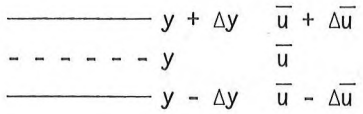

Suppose that n streaks are observed in the band. Roughly n/2 streaks will have a velocity characteristic of position y, while n/4 streaks will have velocities reflecting the top position and n/4 reflecting bottom. Thus the variance owing to velocity gradient will be:

$$S_u^2 = \frac{1}{n-1}\left\{\sum_i^n (\bar{u} - u)_i^2\right\}$$

$$= \frac{1}{n-1}\left\{\sum_1^{n/2} (\bar{u} - \bar{u})^2 + \sum_{n/2}^{3/4n} (\bar{u} - (\bar{u} + \Delta\bar{u}))_i^2 + \sum_{3/4n}^{n} (\bar{u} + (\bar{u} - \Delta\bar{u}))_i^2\right\}$$

$$\simeq \frac{1}{2}(\Delta\bar{u})^2 \qquad (6)$$

If S_m and S_t are the measured and true variances then

$$S_m^2 = S_t^2 + S_u^2 \qquad (7)$$

or

$$\frac{S_t}{S_m} = \left[1 - (\Delta\bar{u}/4S_m)^2\right]^{1/2} \qquad (8)$$

Equation 8 shows the influence of the velocity gradient on the true velocity.

As an example we will consider the first three data points of Run 3. Consideration of the velocity profiles shows this case will have the largest error owing to the above considerations. The $\Delta\bar{u}$ for a band width of 0.0024 inch have been determined directly from the slope of the velocity profile at the indicated radial positions. In the following table, the appropriate data for use in Equation 8 are tabulated.

Table I

Intensity Error Due to the Measurement Technique

No	Y	$\Delta\bar{u}$	S_m	S_t/S_m
	inch	ft/sec	ft/sec	
1	.0040	.18	.567	.95
2	.0073	.13	.508	.97
3	.0102	.04	.535	.97

It is evident from the tabulated S_t/S_m there is little difference between S_m and S_t. For the radial position nearest the wall, where the velocity gradient is the largest, the error would be approximately 5%. In view of the conservative nature of this calculation, it is concluded that for all runs in this work error in intensity because of velocity gradient is negligible.

RESULTS AND DISCUSSION

The summary of the operating conditions of the photographic runs are presented in Table II. The range of values reported for the friction velocity u^* correspond to pressure drop measurements taken at the beginning and end of each photographic run.

Pressure Drop Measurements

Figure 3 represents the friction factor-Reynolds number data obtained for both water and polymeric solutions in the 1-in. and 2.75-in. diameter pipes. Viscometric measurements on the polymer solutions indicated it behaved as a Newtonian fluid with kinematic viscosity of 1.2×10^{-5} ft^2/sec at room temperature (23). The experimental values of the friction factor for water were obtained in order to check the experimental equipment as well as the Newtonian form of the similarity law. The large triangles indicate the photographic runs. As noted from the triangles, drag reduction of up to 60% could be obtained in the 1-in. pipe and of 44% in the 2.75-in. pipe. The available flow rate of the system prevented runs at N_{Re} 114000 in the 2.75-in. pipe while degradation caused by high shear of the system limited readings in the 1-in. pipe. The prediction of drag reduction in the 2.75-in. pipe from the 1-in. pipe data points using a logarithmic similarity law (24) agreed well with the experimental friction data.

Instantaneous Velocities and Analysis of Histograms

In order to show that the number of instantaneous velocities used to estimate the mean velocities was adequate, the cumulative means of axial and radial velocities were considered for each run. As an example, Figure 4 shows the decrease in variability as the number of readings is increased. Large fluctuations of the cumulative mean are observed when less than 10 velocities are used, but become negligible for 30 or more observations. Similar results are predicted from simple statistical analysis.

Typical cumulative axial and radial intensities (normalized with respect to centerline velocity) are plotted in the same manner and shown in Figure 5. It is seen that the curves tend to a stationary value rather slowly as shown, in particular, by the top curve in Figure 5. Consideration of other runs with as many as 200 observations shows that the change in the intensity after 70 observations is insignificant. Again, simple statistics predict that many more observations are necessary to estimate a variance than a mean. Uncertainty limits for the time average velocities were estimated to be within less than 5% at 95% confidence for the bulk of the measurements. The confidence interval for variance is substantially larger as shown by the χ^2-95% confidence intervals in the last column of Table III.

Histograms of instantaneous velocities for both water and 0.01% Separan solution (Run 4 and Run 5), at approximately the same Reynolds number, are given in Figure 6 and Figure 7 for axial and radial velocities, respectively. Although some of these suggest a binodal structure as observed by Popovich (21), insufficient observations have made made to clearly define the distributions. Recent laser measurements equivalent to the ones reported herein but with a larger sample size do not suggest a binodal structure (6).

In order to show the detailed nature of the axial instantaneous velocity distributions inside the boundary layer the distributions of axial velocity have been split according to the sign of the radial component and are shown in Figure 8 for Run 5. Statistics of the conditionally sampled axial velocities are tabulated in Table III for Runs 4 and 5. Thus, for example, for Run 5 at the position nearest the wall 43 observations of velocity were made. Ten of these were streaks moving toward the center (negative) with mean in the axial direction of 1.69 ft/sec and 33 were moving toward the wall with mean of 2.41 ft/sec. In general, although the statistical significance is low, the mean of observations with positive radial velocity is the larger of the two. This is in agreement with the arguments, in Figure 1 that the ejections originate from regions of low momentum fluid (2,7,13,14). Splitting of the distributions for flow in the core region did not show a systematic difference between the means of the axial velocities associated with positive and negative radial velocities.

Table II

Summary of Photographic Runs

Run No.	Fluid	Pipe ID in	$\langle \bar{u}_x \rangle$ ft/sec	U* ft/sec	N_{Re}	f x 10^5	% Drag Reduction
1	water	1.00	4.83	0.259-0.259	38123	550	0
2	water	1.00	3.07	0.175-0.175	23785	620	0
3	0.01%	1.00	4.36	0.189-0.189	-	380	34.5
4	water	1.00	4.98	0.261-0.261	42229	540	0
5	0.01%	1.00	4.98	0.183-0.195	34377	297	48.3
6	water	1.00	13.26	0.624-0.624	104299	450	0
7a	0.01%	1.00	11.62	0.346-0.346	80354	179	62
7b	0.01%	1.00	11.62	0.361-0.361	80354	193	61.2
8	water	2.75	5.00	0.233-0.233	114083	435	0
9	0.01%	2.75	5.07	0.183-0.183	97774	258	43.7

Table III

Conditional Sampling of Axial Velocity

Run	Y^+	Number of Observations	(n)	$\bar{u}_x$ ft/sec	s_x ft/sec
4	13.5	total	22	2.99	0.65 < 0.85 < 1.21
		positive radial	16	2.78	
		negative radial	6	3.07	
4	23.3	total	31	3.57	0.48 < 0.60 < 0.80
		positive radial	19	3.58	
		negative radial	12	3.57	
4	32.2	total	34	3.60	0.37 < 0.45 < 0.575
		positive radial	14	3.69	
		negative radial	20	3.53	
5	10.2	total	43	2.24	0.62 < 0.74 < 0.92
		positive radial	33	2.41	
		negative radial	10	1.69	
5	22.3	total	48	3.35	0.61 < 0.72 < 0.90
		positive radial	36	3.49	
		negative radial	12	2.92	
5	32.9	total	79	3.88	0.61 < 0.71 < 0.84
		positive radial	46	3.95	
		negative radial	33	3.78	

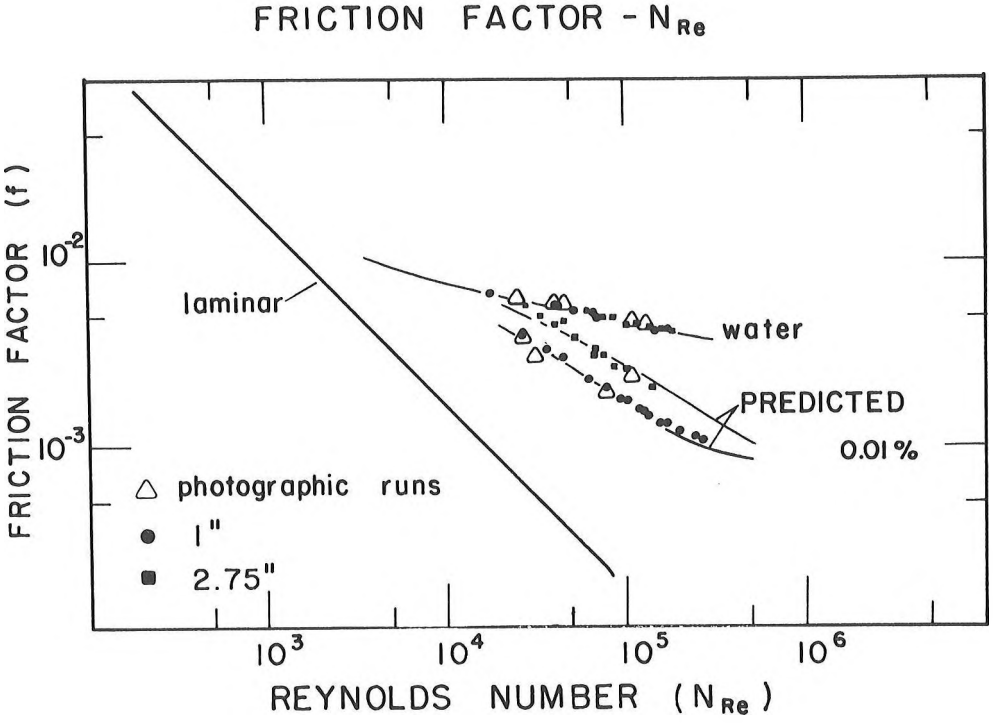

Figure 3. Friction Factor - N_{Re}

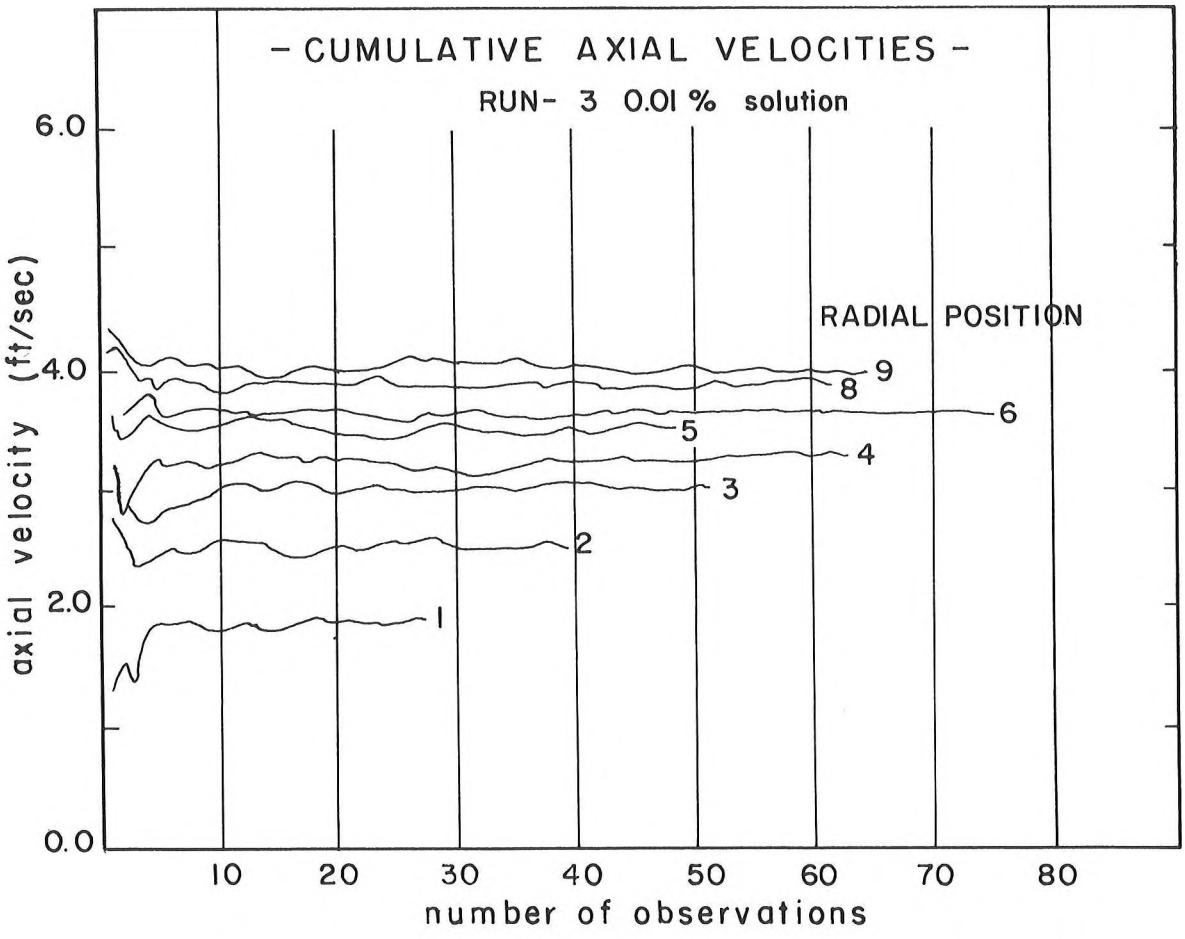

Figure 4. Cumulative Axial Velocities

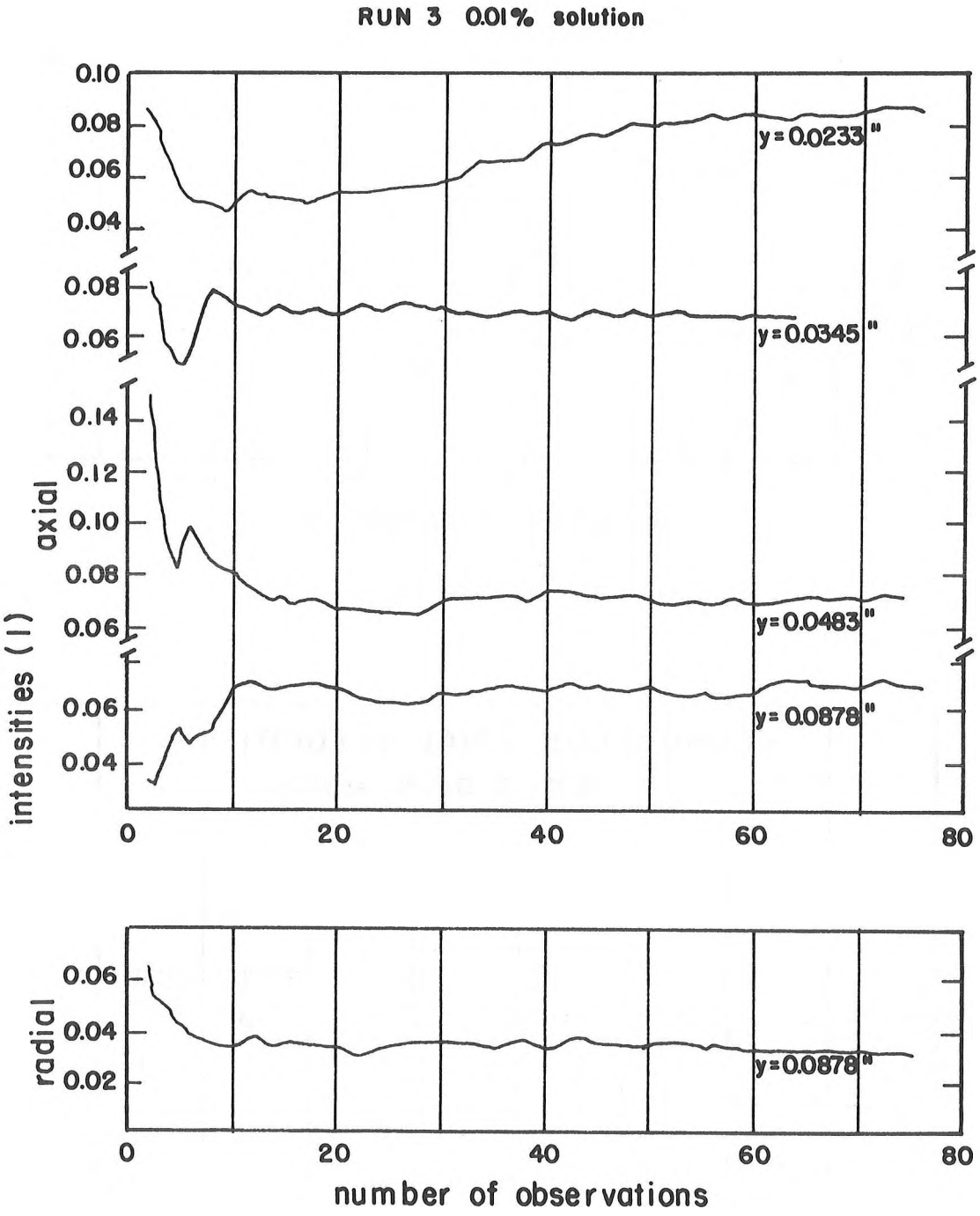

Figure 5. Cumulative Intensities

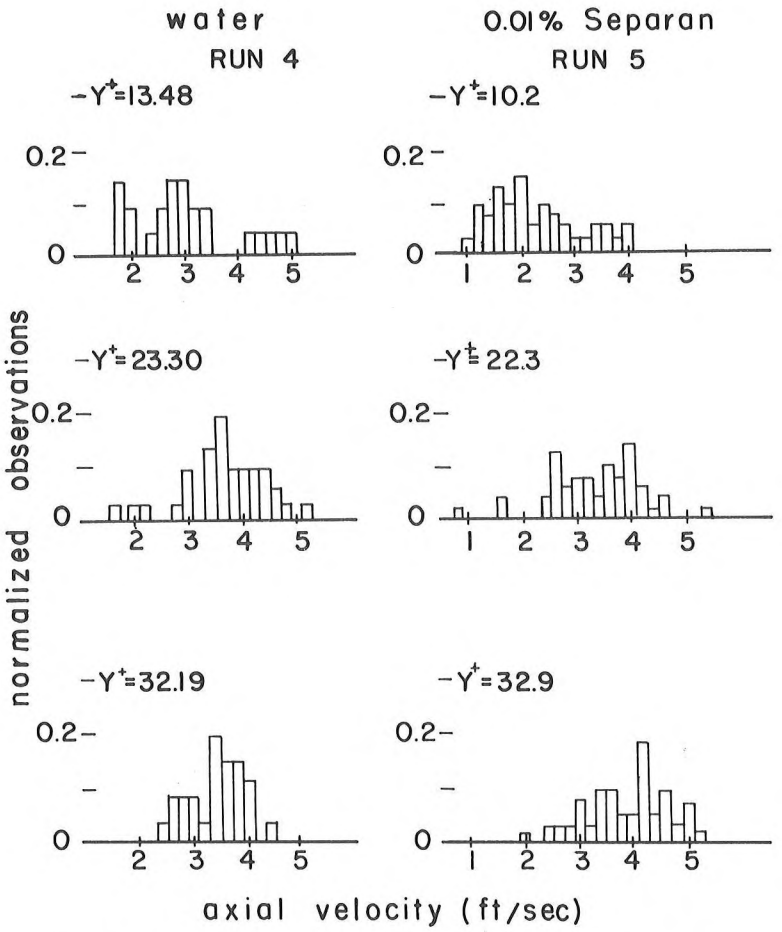

Figure 6. Histograms of Axial Instantaneous Velocities

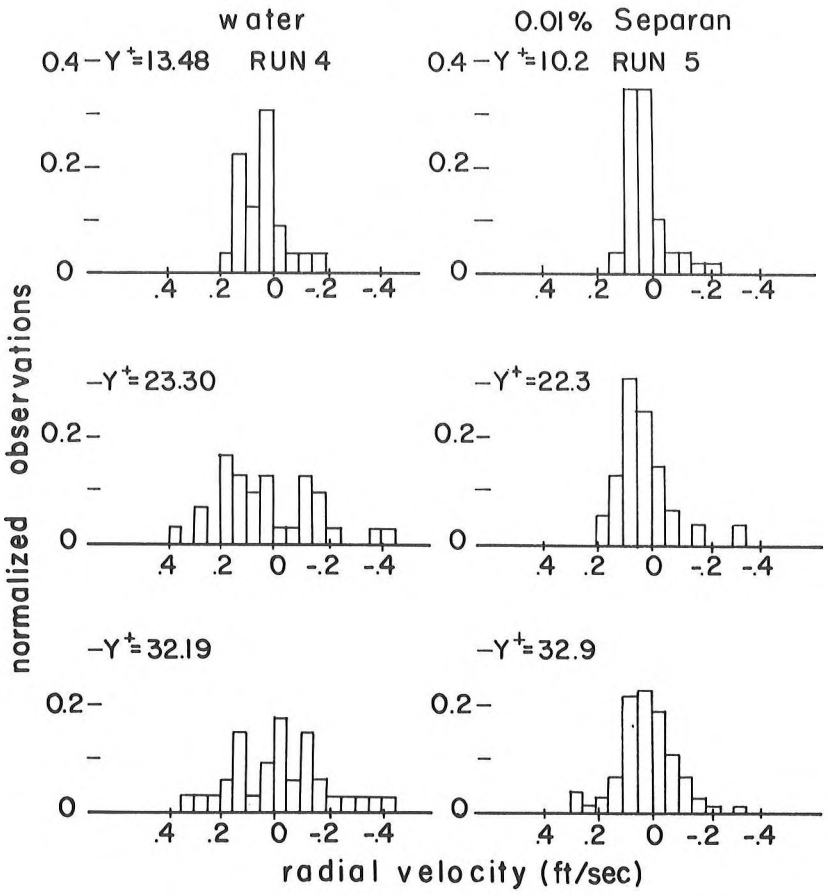

Figure 7. Histograms of Radial Instantaneous Velocities

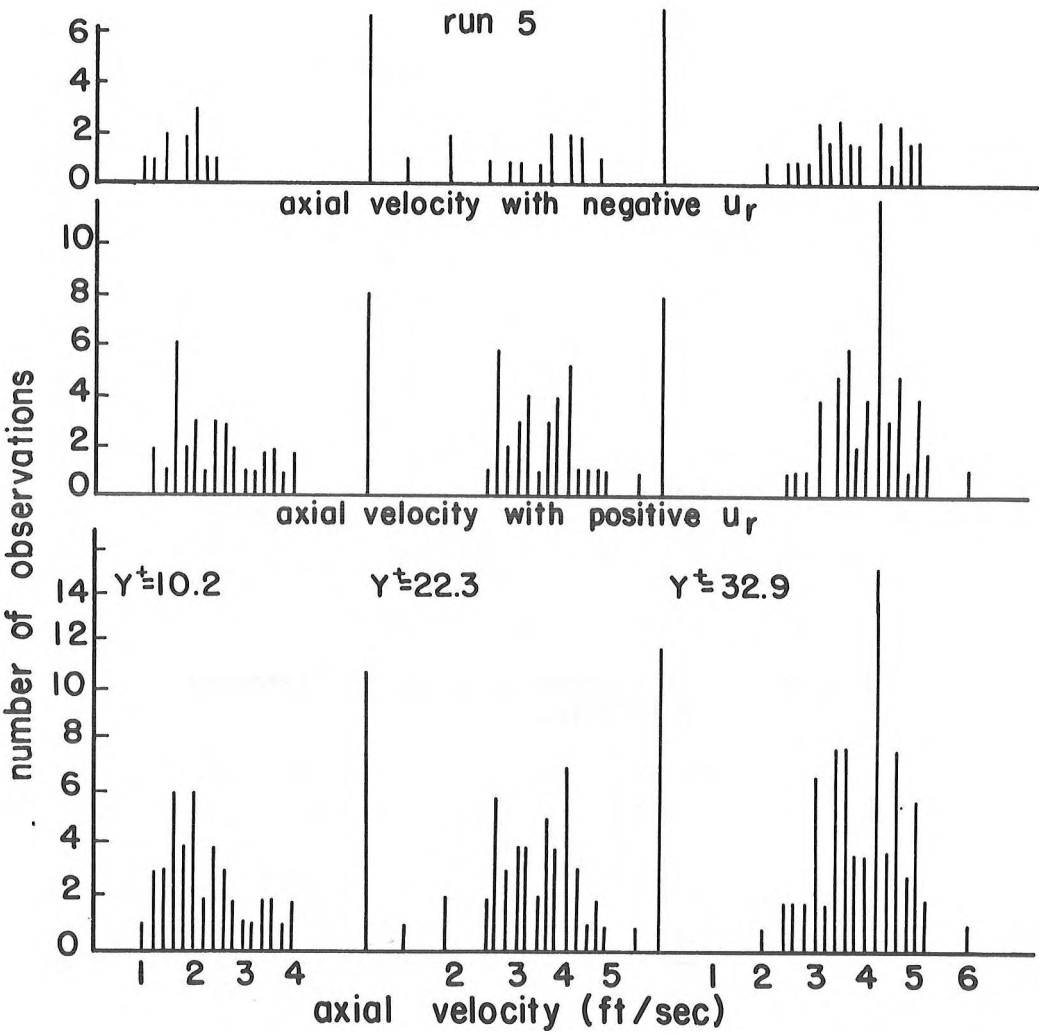

Figure 8. Axial Histograms

Correlation Factor

Values of the correlation factor R_o, defined in Equation 2, are presented as Figure 9 for Runs 3 and 5 of the dilute polymer and Run 4 for water. Data for the other runs, which have been omitted to clarify the figure, show similar behavior. Although there is considerable scatter in the data, there are distinct trends with radial position. As discussed earlier, the bursting arguments coupled with simple continuity considerations, imply R_o should be greater than unity in the vicinity of the edge of the sub-layer. The data points for the water (connected with the dashed line) although not extending deeply enough into the sublayer, suggest this trend. To map the trend completely, one would like measurements for $Y^+ < 10$ (the position where the ejection originates). For example, for water, the data point closest to the wall ($Y^+ \simeq 14$) has an R_o of approximately 3. At this position positive radial fluctuations are observed three times as often as the larger negative fluctuations, while the mean of all the observed fluctuations is zero within the statistical uncertainty of the calculations.

For the polymer solutions there is a distinct peak in values of R_o at $\xi \simeq 0.05$. The values become constant at about $\xi = 0.1$. Consideration of the velocity profiles shown in a previous publication (24), indicates, as expected, that this peak is within the sublayer and the end of the peak ($\xi \simeq 0.1$) coincides with the outer edge of the sublayer which has been shifted to about $Y^+ = 100$. Qualitatively the bursting arguments suggest that R_o, in addition to being greater than unity, should show a peak owing to the acceleration of the fluid element as it moves through the sublayer. The value should decrease to unity at the edge of the sublayer as the fluid mixes with the core fluid.

For the remainder of the cross section, for all the runs, R_o scatters around unity, except over a narrow range of radial position near to $\xi \simeq 0.65$, where it is consistently less than unity. Seyer's earlier data (27) show exactly the same trends. However, no explanation can be offered for this behavior.

Turbulence Intensities

The root-mean-square values obtained for each set of the axial and radial instantaneous velocities are used to estimate the relative turbulence intensities. As indicated in reference (23), a survey of the measured relative intensities in drag reducers leads to confusion owing to the uncertain accuracy of the results and how to scale or compare them for the different systems.

Figure 10 shows the intensity data (relative to the maximum velocity) for the water Run 4 and Figures 11 and 12 show the velocity and intensity profiles for the polymeric solution Run 5. The solid curves on the intensity figures represent Sandborn's data (25) for air at the indicated Reynolds numbers. In each case the lower curve is radial and the upper is axial intensity. For the water run, the data show reasonable agreement with Sandborn's curve over the entire cross-section.

The 0.01% Separan relative intensity with the uncertainty intervals shown for Run 5 in the 1-in. tube are compared at approximately equal Reynolds numbers to the air curves. Since the water and the polymer viscosities are about the same, the comparison could also be viewed as one at the same flow rate or bulk average velocity.

For the data shown and other runs the radial intensities are markedly lower, at all radial positions, than the intensities for Newtonian fluids. The amount of lowering of the intensities is ordered according to the amount of drag reduction.

Although the statistical significance is low, axial intensities for the low Reynolds number run shown are not altered significantly from the Newtonian values until y/R values are greater than 0.5. At high Reynolds number, however, the data indicate some lowering of the axial intensity in the core region (23).

In Figure 12 it is of interest to note the increase of radial intensity, associated with the edge of the boundary layer for Newtonian fluids, is shifted toward large radial position. This suggests, in agreement with the velocity measurements, a significant thickening of the boundary layer. This trend was observed with all of the radial intensity data.

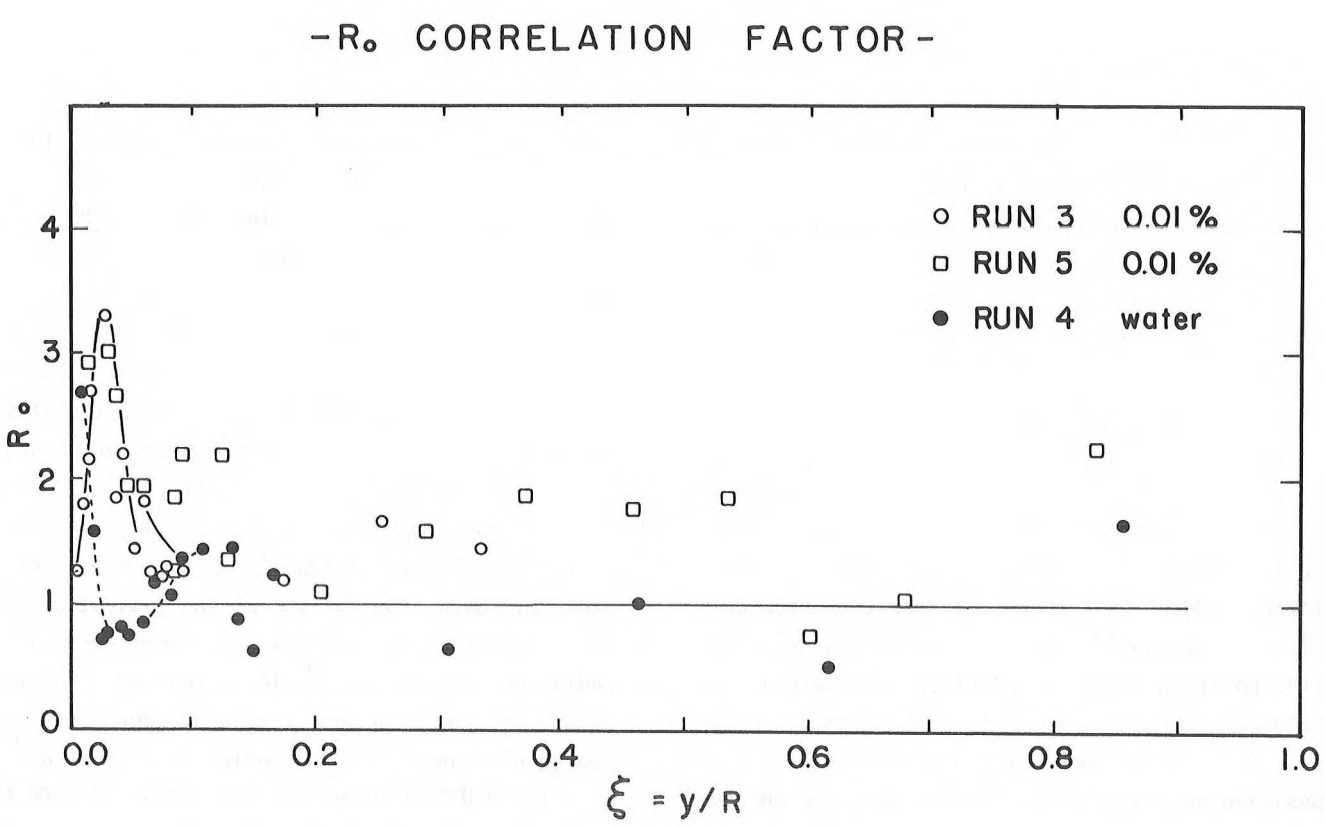

Figure 9. R_o - Correlation Factor

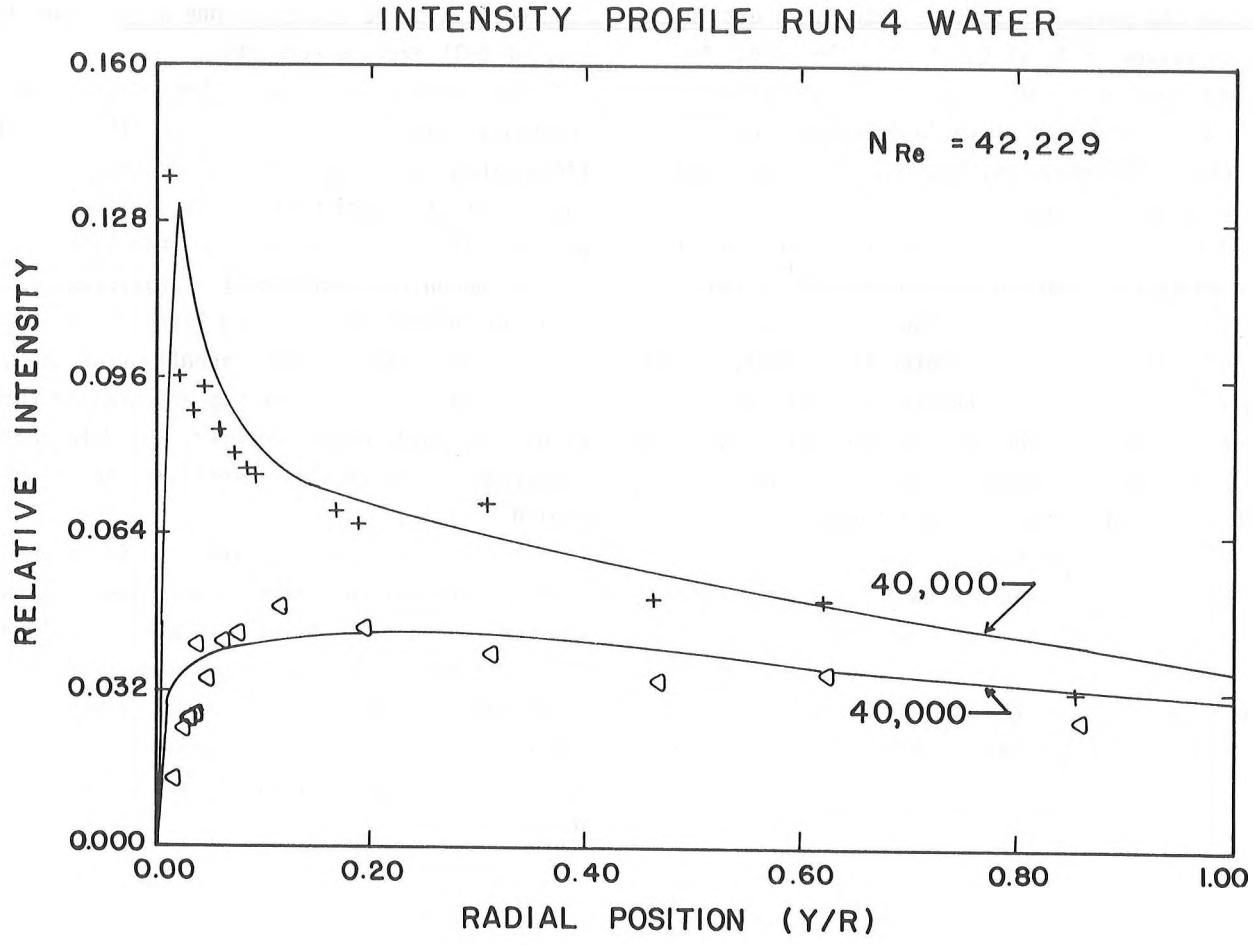

Figure 10. Intensity Profile - Run 4 Water

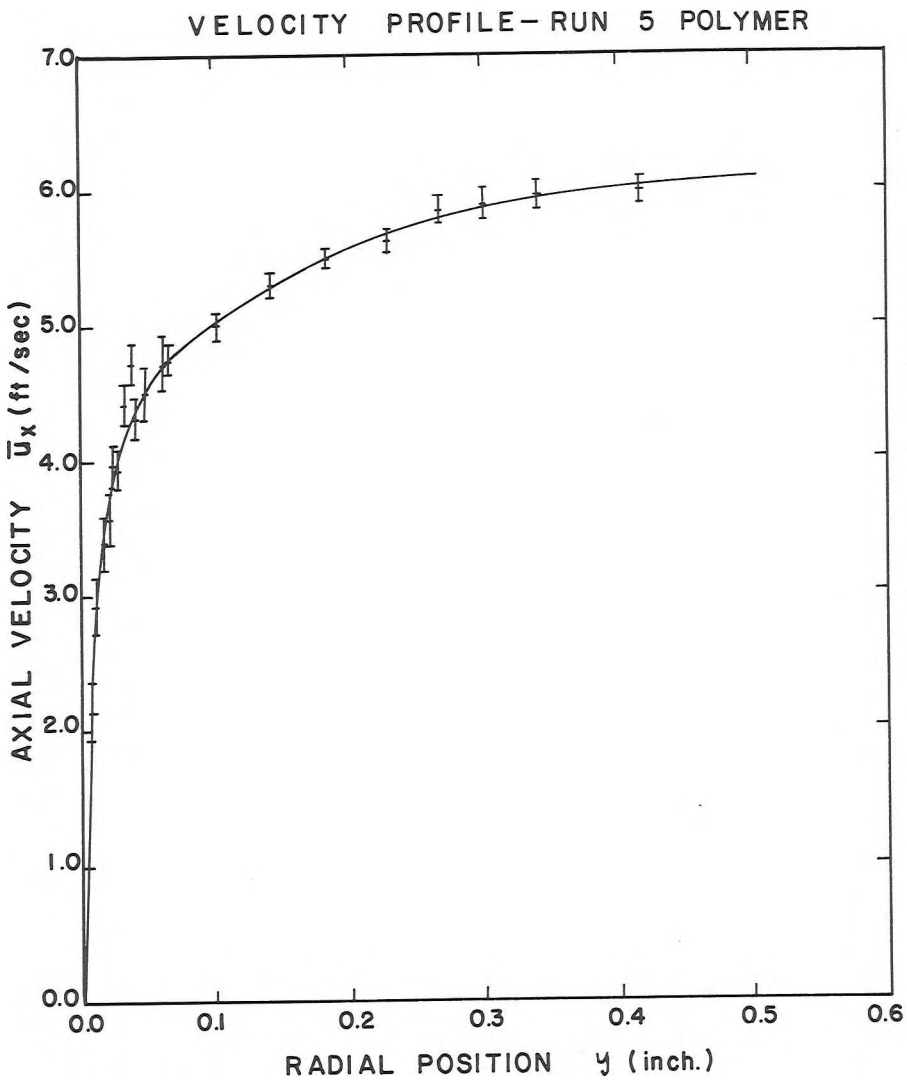

Figure 11. Velocity Profile - Run 5 Polymer

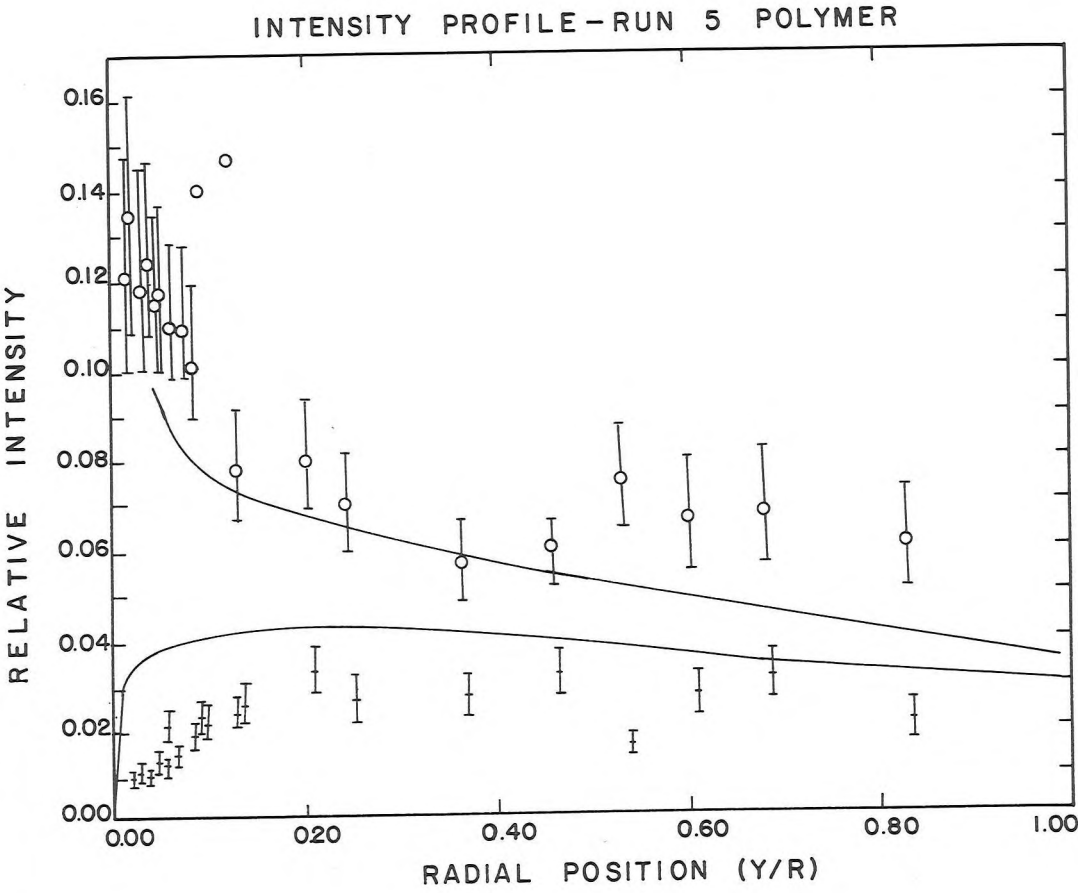

Figure 12. Intensity Profile - Run 5 Polymer

CONCLUSIONS AND SUMMARY

A series of measurements of instantaneous velocity from streak photographs have been obtained in Newtonian and drag reducing fluids. Based on a comparison with available Newtonian data of velocity profiles and axial and radial intensities, the quantitative usefulness of the technique is verified. Since the streak photograph technique does not suffer from the serious limitations of probe devices, it is suggested that the measurements in drag reducing fluids are also quantitatively correct.

By ordering the set of instantaneous velocities according to the sign of the radial component it is found that, in the boundary layer, on the average, the fluctuating velocities toward the center of the tube are larger than those toward the wall. This observation agrees with the visual observations of "bursting" described by Brodkey and others.

For a given radial position, the largest fluctuations in radial histograms for polymer solutions are less than those for Newtonian fluids at similar conditions. A similar conclusion follows from a consideration of the root mean square of the velocities made dimensionless with respect to the maximum velocity.

ACKNOWLEDGMENT

The financial support of NRC and the Dow Chemical Co. who donated the polymer are greatfully acknowledged.

SYMBOLS

D	diameter of the pipe
f	friction factor defined as $\tau_w/1/2\ \rho\langle\bar{u}_x\rangle^2$
L	length between pressure taps
M	number of divisions on the "timing wheel"
n	total number of observations of instantaneous velocities
n^+	number of positive radial instantaneous velocities
n^-	number of negative radial instantaneous velocities
N_{Re}	Reynolds number
r	radial position from center of the pipe
R	radius of the pipe
R_o	correlation factor defined in Equation 2
S_x, S_r	standard deviation of the instantaneous velocities
t	time
T	time scale of a streak [60/M W], in sec.
u_x, u_r	instantaneous velocity components
u'_x, u'_r	fluctuating components of the velocity
$\langle\bar{u}_x\rangle$	bulk velocity
u*	friction velocity defined as $\sqrt{\tau_w/\rho}$
W	rotational speed of the "timing wheel" in RPM
X,Y	coordinate axis on projection screen of digitizer
y	radial position from the wall
y^+	dimensionless distance from the wall defined as $y\ u^*/\nu$
μ	fluid viscosity
ξ	dimensionless distance from the wall defined as y/R
ρ	density of the fluid
τ	shear stress
ν	kinematic viscosity
$(\ )_i$	indicates the i^{th} observation of instantaneous quantity
r	radial direction
x	axial direction or direction of flow in pipe
w	referred to the wall

BIBLIOGRAPHY

1. Bakewell, H. P., and Lumley, J. L., "Viscous Sublayer and Adjacent Wall Region in Turbulent Pipe Flow", Phys. of Fluids, 10, 1880 (1967).

2. Corino, E. R., and Brodkey, R. S., "A Visual Investigation of the Wall Region in Turbulent Flow", J. Fluid Mech., 37, 1 (1969).

3. Denn, M. M., and Marrucci, G., "Stretching of Viscoelastic Liquids", A.I.Ch.E. J., 17, 101 (1971).

4. Denn, M. M. and Porteous, K.C., "Elastic Effects in Flow of Viscoelastic Liquids", Chem. Eng. J., 2, 280 (1971).

5. Donohue, G. L., Tiederman, W. G. and Reischman, M. M., "Flow Visualization of the Near-Wall Region in a Drag-Reducing Channel Flow", J. Fluid Mech., 56, 559 (1972).

6. Donohue, G. L., et al., "Turbulence Measurements with a Laser Anemometer Measuring Individual Realizations", Phys. of Fluids, 15, 1920 (1972).

7. Eckelmann, H., and Reichardt, H., "Experimental Investigation in a Turbulent Channel Flow with a Thick Viscous Sublayer", 2nd Symp. on Turbulence in Liquids, University of Missouri-Rolla, Oct. 1971, Cont. Ed. Ser.

8. Fage, A., and Townend, H. C. H., "An Examination of Turbulent Flow with an Ultramicroscope", Proc. Royal Soc., Ser. A, 135A, 656 (1932).

9. Fortuna, G., and Hanratty, T. J., "The Influence of Drag-Reducing Polymers on Turbulence in the Viscous Sub-Layer", J. Fluid Mech., 53, 575 (1972).

10. Fowles, P. E., "The Velocity and Turbulence Distribution in the Laminar Sublayer", Sc.D. Thesis, Chem. Eng. Dept., M.I.T., (1966).

11. Gordon, R. J., "On the Explanation and Correlation of Turbulent Drag Reduction in Dilute Macromolecular Solutions", J. of Appl. Polymer Sci., 14, 2097 (1970).

12. Hinze, J. O., Turbulence, McGraw-Hill, New York, 1959.

13. Klebanoff, P. S., "Characteristics of Turbulence in a Boundary Layer with Zero Pressure Gradient", NACA Report 1247, 1955.

14. Kline, S. J., Reynolds, W. C., Schraub, F. A., and Runstadler, P. W., "The Structure of Turbulent Boundary Layers", J. Fluid Mech., 30, 741 (1967).

15. Laufer, J., "The Structure of Turbulence in Fully Developed Pipe Flow", NACA TR 1174, 1954.

16. Meek, R. L., and Baer, A. D., "The Periodic Viscous Sublayer in Turbulent Flow", A.I.Ch.E. J., 16, 841 (1970).

17. Millikan, C. B., "A Critical Discussion of Turbulent Flows in Channels and Circular Pipes", Proc. 5th Intern. Congr. Appl. Mech., p. 386, John Wiley, N.Y., 1939.

18. Nedderman, R. M., "The Use of Stereoscopic Photography for the Measurement of Velocities in Liquids", Chem. Eng. Sci., 16, 113 (1961).

19. Nychas, S., "A Visual Study of Turbulent Shear Flow", Ph.D. thesis, Ohio State University (1972) and Nychas, S., et al., J. Fluid Mech., 61, 513 (1973).

20. Patterson, G. K., Zakin, J. L., Rodriguez, J.M., "Drag Reduction: Polymer Solutions, Soap Solutions and Solid Particle Suspensions in Pipe Flow", Ind. Eng. Chem., 61, (1), 22 (1969).

21. Popovich, A. I., "Statistical Analysis of Fluid Flow Fluctuations in the Viscous Layer Near a Solid Wall", I & E.C. Fund., 8, 609 (1969).

22. Popovich, A. I., and Hummel, R. L., "Experimental Study of the Viscous Sublayer in Turbulent Flow", A.I.Ch.E. J., 13, 854 (1967).

23. Rollin, A., "Similarity Laws and Turbulence Structure of Drag Reducing Fluids", Ph.D. Thesis, University of Alberta, 1971.

24. Rollin, A., and Seyer, F. A., "Velocity Measurements in Turbulent Flow of Viscoelastic Solutions", The Can. J. of Chem. Eng., 50, 714 (1972).

25. Sandborn, V. A., "Study of the Momentum Distribution of Turbulent Boundary Layers in Adverse Pressure Gradients", NACA TN 3266, 1955.

26. Savins, J. G. "Contrasts in Solution Drag Reduction Characteristics of Polymer Solutions and Micellar Systems", Viscous Drag Reduction. ed. by C. S. Wells, Plenum Press, N.Y., 1969.

27. Seyer, F. A., "Turbulence Phenomena in Drag Reducing Systems", Ph.D. Thesis, Chemical Engineering Department, University of Delaware, 1968.

28. Seyer, F. A., and Metzner, A. B., "Turbulence Phenomena in Drag Reducing System", A.I.Ch.E. J., 15, 426 (1969).

29. Townsend, A. A., The Structure of Turbulent Shear Flow, Cambridge University Press, 1956.

30. Wells, C. S., and Spangler, J. G., "Injection of a Drag-Reducing Fluid into Turbulent Pipe Flow of a Newtonian Fluid", Phys. of Fluids, 10, 1890 (1967).

DISCUSSION

M. M. Reischman, Oklahoma State University: I have two comments to make. First of all two years ago at this same conference Eckelmann in conjunction with Reichardt presented a paper that showed quite an extensive histogram distribution throughout the flow in an oil channel that showed no binodal distribution that I recall. We have shown the same thing in very recent experiments at Oklahoma State and as a matter of fact for y^+ less than 50, Reynolds numbers less than 50,000, we show with 400 samples no binodal distribution at all. There appears to be a contradiction. Secondly, the fact that the dilute polymer solution does not have binodal distributions could be the result of the fact that it has a narrower band -- that is, a narrower spread in the histogram itself. The number of data points per unit width of the histogram is then higher and you have less chance of having the kind of scatter that would give you a binodal distribution.

R. S. Brodkey, The Ohio State University: How many points do you actually use? You used about 20-30 for the mean, which is reasonable. I thought 70 was pretty low for an intensity, but how many were actually used in the histogram plot? I would venture to say that the number is an order of magnitude low for a probability density distribution. I would think you would need several thousand. There are two works of interest - Gupta and Kaplan have the probability density distribution for the U- and V- velocities measured with large sample sizes and there is no indication of binodal characteristics. Eckelmann had only U-data and there was no binodal indication. Eckelmann, Wallace, and Brodkey had U- and V-velocities and confirm once again that there is no binodal distribution. In this later work, 128,000 data points rather than 300 or 400 were used. This is the same criticism that was made of the original Popovich and Hummel work.

W. G. Tiederman, Oklahoma State University: Two comments, one is related to this question, of how many points you need. We do individual-realization laser anemometry at our place and about 18 months ago in the Physics of Fluids there were some estimates of how many statistically independent realizations you need in order to get a certain uncertainty in a mean. For example, at a y^+ of 10 for plus or minus 5% at the 95% confidence interval you need 144 points. This is based on standard statistical techniques and is relatively straightforward, and you need quite a bit more than that if you're going to do intensity, so I would also criticize this technique of looking for when the additional realization no longer effects your accumulation up to that point. It, of course, won't affect it very much at all if you start out having some realizations right at first of what is eventually going to be the mean. This is very dramatic because when you go to the center line the number drops to two. So it also depends on how you split up that horizontal axis when you do the histograms. I suspect the binodal thing is not statistically significant.

Rollins: I agree with you on the number, but if the mechanism proposed is O.K., we should have a longer actual component from the loop of fluid coming in relative to the one going into the center.

Tiederman: I think that would only be true if you were conditionally sampling in an appropriate way. I don't think it is true if you sample over a long time.

Seyer*: I agree with the general criticisms of the weak statistical significance in a formal sense of most of our results, especially near the wall. In particular the suggested binodal nature of the histograms has no statistical significance. On the other hand the ordering of the data that we have done by separately looking at velocities associated with flow towards and away from the wall consistently show effects which are in agreement with the simple physical picture. Since the observations have been done at several flow rates, several radial positions, and in two different tubes it would be nonsense to argue that the effects we observe are statistical accidents.

---

*Comment added in press.